Award Number G14AP00012

Post-1 Ma Deformation History of the Pitas Point-North Channel-Red Mountain Fault System and Associated Folds in Santa Barbara Channel, California

Authors: **Christopher C. Sorlien** (P.I.) and Craig Nicholson
Previous NSF-funded project with Richard Behl and James Kennett
Additional contributions from Courtney Marshall and Marc Kamerling
(Only Sorlien was funded by G14AP00012).

Report date October 07, 2015.

Sorlien: Earth Research Institute
University of California, Santa Barbara
email: christopher.sorlien@ucsb.edu
Home office phone in Rhode Island: 401-560-0368

Nicholson: Marine Science Institute, University of California, Santa Barbara
Email: craig.nicholson@ucsb.edu
Phone: 805-893-8384

Term of award: January 1, 2014 – June 30, 2015

"Research supported by the U.S. Geological Survey (USGS), Department of the Interior, under USGS award number G14AP00012. The views and conclusions contained in this document are those of the authors and should not be interpreted as necessarily representing the official policies, either expressed or implied, of the U.S. Government."

ABSTRACT

Identification of the problem and implications

The north margin of rapidly-shortening, rapidly-subsiding offshore and onshore Ventura Basin is comprised of major N-dipping faults. Evidence for 6 to 8 meter uplift events near Ventura have been linked to proposed paleo-quakes approaching Magnitude 8.0 on these faults. However, it has become controversial whether these uplift events are representative of the 120 km-long offshore part of the fault system west of Ventura The 3D geometry of the western 60 km of the fault system has not been known, especially at a few km depth. Therefore, it has been unknown whether there are geometric segment boundaries important enough to form rupture barriers.

The current shortening derived from GPS data and the total post-Miocene shortening derived cross sections both indicate lower total shortening to the west. It is not known whether the lower cumulative shortening in the west is due to slower rates of shortening, propagation of initiation of shortening from east to west, or both. The major question then becomes to what extent is the mapped geometry of active faults, and the observed rates of shortening across these faults consistent with the proposed models of multi-segment ruptures and large magnitude, tsunamigenic earthquakes?

Summary of Approach

Ten dated stratigraphic horizons ranging in age from 1,800 ka to 110 ka and many fault strands were interpreted on ~700 deep-penetration industry multi-channel seismic reflection (MCS) profiles, high resolution MCS profiles, and 3D MCS volumes. Bathymetry, and well and core data with paleontology were utilized. The interpretation includes on the order of 100,000 horizon and fault "ties" at MCS profile intersections ("loop tying"). The interpretations of faults and the stratigraphic horizons have been gridded and depth-converted using velocity surveys in >3 dozen wells. Deformation that occurred during the different intervals of time has been recorded by folding; folding is documented by 3D depth-converted grids of many precisely-dated stratigraphic horizons. Combining the digital folded horizons with the digital 3D faults provides powerful constraints on models for earthquake slip and uplift.

Results

The N-dipping North Channel-Pitas Point-Red Mountain (NC-PP-RM) fault-fold system continues 120 km west of Ventura. The lowest main interpreted fault strand, the Pitas Point - Ventura fault, has no significant geometrical discontinuities in its upper few km for 60 km west of Pitas Point. There is a segment boundary and a 25° bend in strike 10 km west of UCSB. Left-lateral slip is likely more important west of this bend. The lower faults of the whole 120 km-long offshore system are blind, with sea floor/surface deformation expressed by folding, not fault offset. Some of the blind fault strands do not appear to have propagated updip during the last few hundred kyr, producing progressive tilting of the forelimb. Such fault-related folds produce a completely different pattern of shallow slip and sea floor uplift than is the case for propagating faults that do not produce tilting of the forelimb.

The timing and pattern of folding of the 10 interpreted stratigraphic horizons allows discrimination between models for lateral westward propagation of (oblique) thrust faulting, vs. just slower deformation in the west. The offshore post-1.8 Ma shortening and shortening rates through present due to folding and fault slip both decrease westward from SE of Santa Barbara to beyond Point Conception. Published cross sections and the MCS data indicate that the initiation of contraction long predates deposition of a 1.8 Ma horizon. Therefore, total contraction is less in the west because it has long been slower, not because it is younger. Either multi-segment ruptures affecting the fault system west of Santa Barbara are rarer than earthquakes affecting the east, or the slip per event decreases to the west.

1: **Introduction**

Ventura Basin is a rapidly-subsiding arcuate basin, bounded by outward-dipping reverse faults and oblique reverse faults. The northern, N-dipping faults include the San Cayetano fault, and numerous fault strands that comprise the North Channel-Pitas Point – Red Mountain fault system (Fig. 1)[Kamerling et al., 2003; Fisher et al., 2009]. The Ventura basin continues offshore for about 80 km, beyond where its southern structural boundary becomes more subdued and the basin is much wider. GPS shortening across Ventura basin is about 7 mm/yr east of the longitude of Santa Barbara [e.g., Marshall et al., 2013].

Repeated 6 to 8 m uplift events at Pitas Point, just west of Ventura, can be interpreted from paleo-beaches capped by middens [Gamble, 1983, Rockwell et al., 2014]. Large uplift events were also interpreted from lines of closely-spaced core holes within the northern part of Ventura [McAuliffe et al., 2015]. It is not known whether these events occurred in single major earthquakes or partly or largely over a period of subsequent months. It has also become controversial whether these uplift events are produced exclusively as a result of slip on the N-dipping faults, and whether they are representative of the 120 km-long offshore part of the fault system west of Ventura [e.g., Nicholson et al., 2015]. Uplift events that large are theoretically expected to be due to earthquake near M8, based on slip-fault length relationships [e.g., Scholz, 1990]. Owing to the uncertainty and possible increased hazard, the Southern California Earthquake Center established a Special Fault Study area for the active fault systems bounding onshore and offshore Ventura basin.

A paper was published in 2014 proposing that these uplift events occurred during earthquakes of Magnitude 7.7 to 8.1 [Hubbard et al., 2014]. These authors produced a representation of the onshore part of the N-dipping Pitas Point -Ventura fault based on petroleum well data, and limited seismic reflection imaging [Hubbard et al., 2014]. The fault geometry derived from onshore data was then projected/extrapolated 30 km offshore to Santa Barbara [Hubbard et al., 2014]. This new addition to the SCEC CFM, the N-dipping extrapolated upper ramp fault geometry from Hubbard et al. [2014], was used for dynamic rupture and tsunami modeling of a M7.7 offshore thrust earthquake, with average slip of 7.4 m and maximum slip near 15 m, with more than 10 m of slip locally reaching the sea floor [Ryan et al., 2015]. Sea floor uplift reaches 7 m in that model earthquake, and model tsunami runup from the model quake affects 1 to 2 km inland, south of Ventura [Ryan et al., 2015].

Earthquake hazard is, among other things, related to the Holocene slip rate on faults, which can be related to GPS strain accumulation, but does not have to be. For example, some GPS measurements may be related to non-elastic strain accumulation unrelated to earthquake generation [Nicholson et al., 2007], and other GPS-measured strain accumulation has been shown to be transitory in California [e.g., Dolan et al., 2007]. The continuity of faults is related to the likely maximum magnitude of earthquakes, and given some long-term rate of deformation, to the average recurrence interval. Earthquakes can rupture multiple segments, but the nature of the segment boundary and the type of fault slip across a boundary would seem important to the probability of multi-segment earthquakes.

The Santa Ynez Mountains are located between the deep North Channel-Pitas Point-Red Mountain fault system to the south and the Santa Ynez fault system to the north. Their elevation decreases from near the UCSB campus steadily westward. The dips of sedimentary rocks in the southern limb of these mountains also decrease to the west [e.g., Dibblee, 1950, 1966]. The post-1.8 Ma shortening across the offshore fault-fold system also decreases westward between Santa Barbara and UCSB [Sorlien and Kamerling, 2000]. Lower total shortening can be explained by lower rates of shortening through the last 1.8 Ma or longer, or by a shorter duration of shortening at a higher rate, or to both. If contraction has propagated from east to west through time, the duration of shortening would be less in the west. Current shortening modeled from GPS data also decreases westward [Marshall et al., 2013], suggesting but not requiring that Holocene slip rate for the thrust component decreases westward.

Fault representations in the SCEC Community Fault Model [Plesch et al., 2007] indicate discontinuities in the shallow faulting that may limit the expected magnitude of earthquakes on this system. Does the development of, and shortening across the regional fault system over the last 1 Myr suggest multiple segment ruptures and major quakes? Here, we provide information on the actual geometry of the upper 6 km of the fault strands, and the geometry and history of the folding for the last 1 Myr.

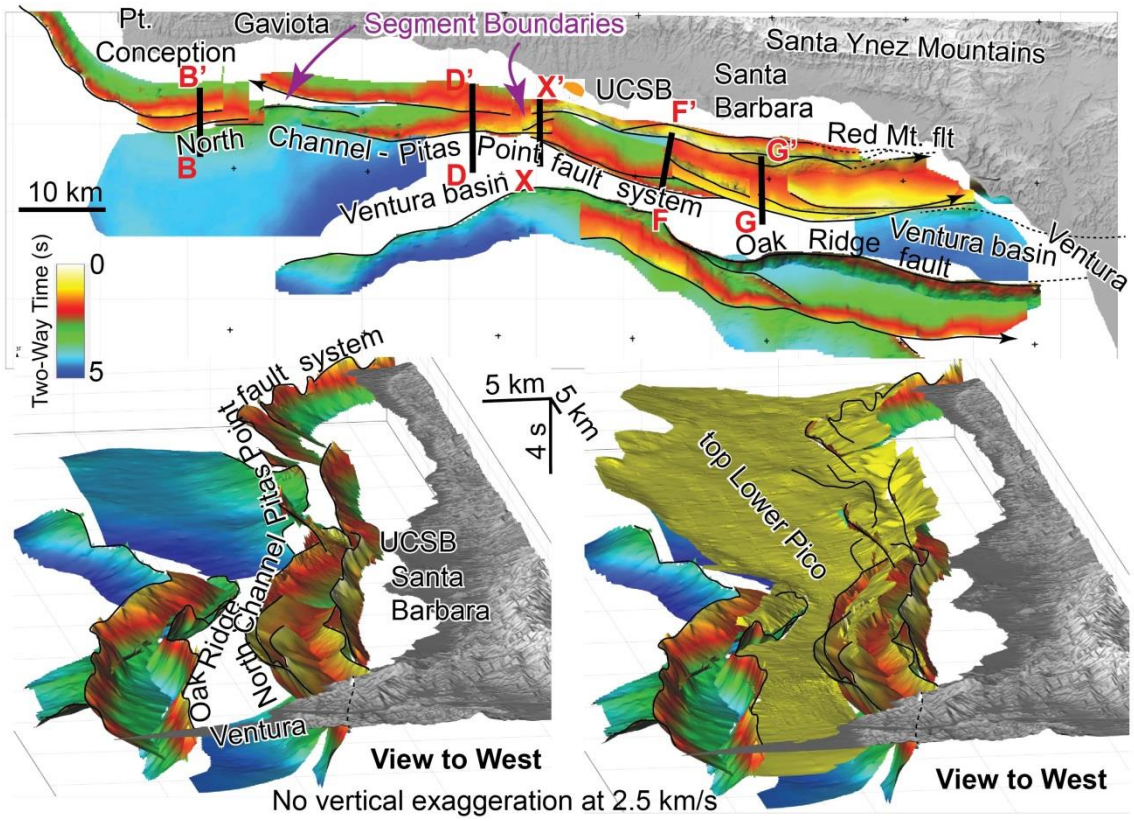

Figure 1: Plan and oblique views of newly-interpreted faults in Santa Barbara Channel, displayed in two-way time. Seismic reflection profiles in later figures are located. Lower right: Includes mapped 1.8 Ma, top Lower Pico stratigraphic reference horizon, yellow.

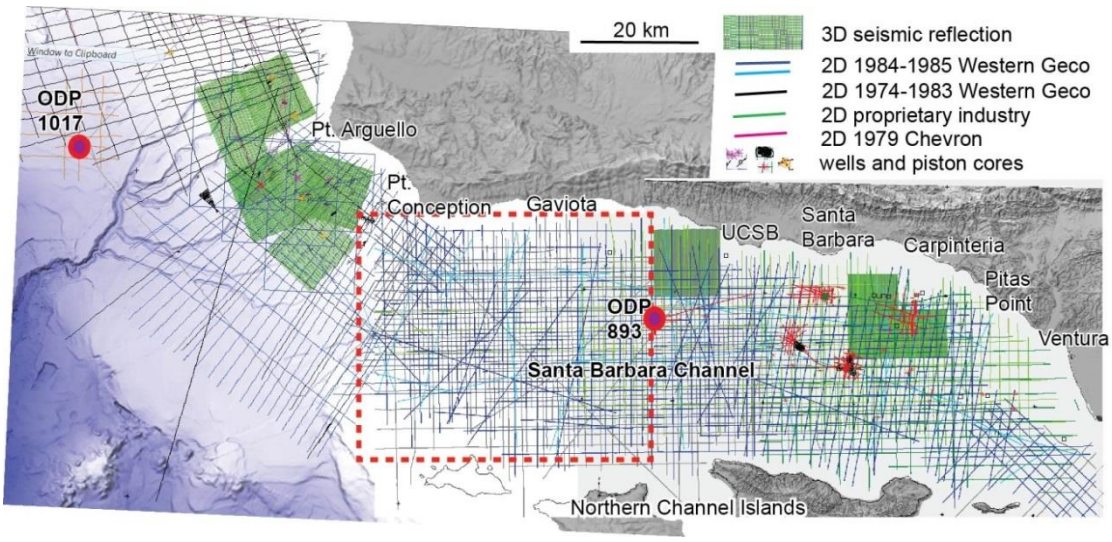

Figure 2: Basemap of 750 2D seismic reflection profiles and three 3D surveys used in the interpretation and gridding of nine 975 ka and younger horizons, and a 1,800 ka horizon. An additional five digital 3D surveys are part of the Kingdom Suite project northwest of Pt. Conception, as well as numerous additional 2D profiles. Wells and piston cores are shown by small symbols; 8 additional wells and their velocity information have been added within the red dashed box but are not on this figure. The non-proprietary part of this project including fault and horizon interpretations for the whole area of the red dashed box was added to another Kingdom Suite project covering from Pt. Conception to Monterey Bay. This combined project was provided to USGS-Santa Cruz during June 2015. There are 2,500 line intersections within that box, so 25,000 "ties" for the ten horizons have been made just there.

2: Data and Methods of Analysis

2.1: Data Sources

Industry multichannel seismic reflection data (MCS) acquired by Western Geophysical, Chevron, and Jebco, during the mid-1970s through the 1980s were made publicly available in recent years through the National Archive of Marine Seismic Surveys [Hart and Childs, 2005; http://walrus.wr.usgs.gov/NAMSS/index.html] (Fig. 2). The industry data in Santa Barbara Channel are exclusively provided to NAMSS by Western Geophysical, although GSI acquired one of these data sets in 2005. We converted one entire still-proprietary seismic reflection survey from the 1980s from paper to SEGY, involving scans and time-consuming use of the software ImageToSEGY. This involved 100 profiles and profile segments. This data set was the main (but not only) MCS data used for the previous 3D interpretation of the fault system [Kamerling et al., 2003], that was later incorporated into the SCEC Community Fault Model [Plesch et al., 2007]. Three 3D MCS data volumes across the North Channel Pitas Point faults system were also loaded into the Kingdom Suite project and interpreted. These 3D surveys were provided by the USA Bureau of Safety and Environmental Enforcement (BSEE, formerly part of the USA Minerals Management Service (MMS)). An additional five 3D surveys are part of the interpretation project northwest of Pt. Conception: one of these was interpreted across the western end of the North Channel-Pitas Point fault system. Acquisition of all these profiles and volumes was designed to image deeply (5-6 km) and over a broad area in order to fully characterize the petroliferous Miocene section. Higher resolution single channel reflection

profiles shot by the USGS in 2002, 2005, and 2008 were also utilized [e.g., *Sliter et al.*, 2008, Nicholson et al., 2006], as were high-resolution multichannel profiles we acquired in 2008 [Nicholson et al., 2008; Marshall, 2012]. (http://www.ngdc.noaa.gov/mgg/bathymetry/). Multibeam bathymetric data from *MBARI* [e.g., Eichubl et al, 2002], and the USGS [Dartnell et al., 2005] were utilized, and a regional 100 m grid that incorporates those data and point data was created using GeoMapApp [Ryan et al., 2009] High resolution multibeam bathymetry, backscatter, and sparker and chirp seismic reflection located across the northern few km of Santa Barbara Channel were locally utilized [Johnson et al., 2013, 2014, 2015]. Finally, we have tiff files of 25,000 offshore west coast well logs, provided by MMS (now BSEE and Bureau of Ocean Energy Management (BOEM). For our 2014-2015 work, information from >3 dozen of these wells was mainly used for the 3D velocity model and depth conversion. Many of these wells drill through the main strands of the North Channel-Pitas Point fault system, as well as through the Hobson thrust (Padre Juan fault system) [Edwards, 1998; Heck and Edwards, 1998; Redin et al. 2005].

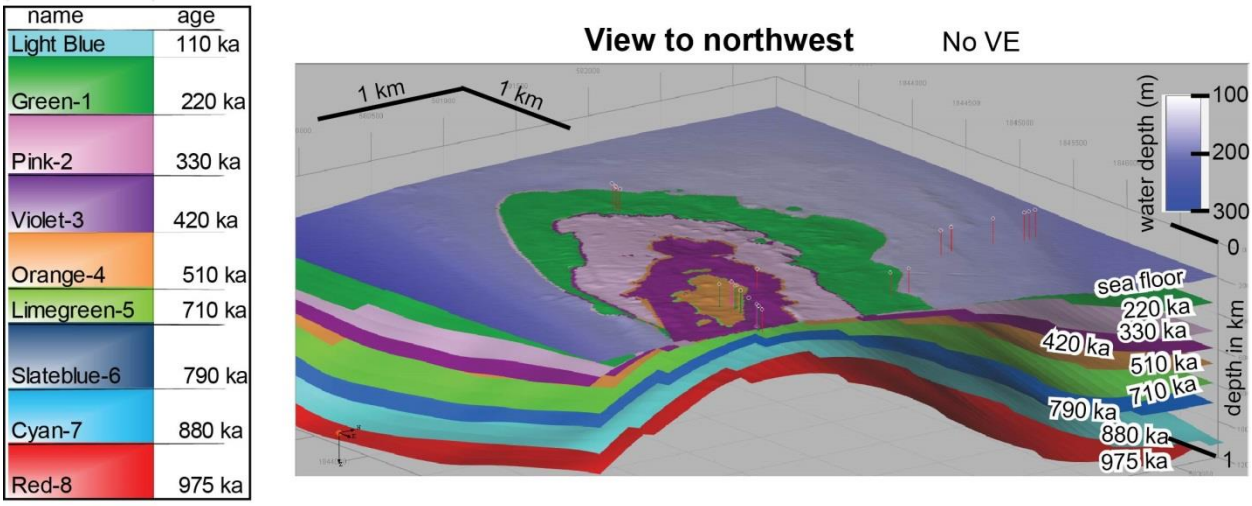

Figure 3: Left: Santa Barbara basin chronostratigraphy [Behl et al., 2011; Marshall, 2012]. Right: Sea floor through 975 ka horizons along the Mid Channel anticline. Small dots and lines are piston cores from 2005 and 2008 that sample dipping strata that sequentially outcrop at the sea floor [e.g., Nicholson et al., 2006]. Dating incorporated a previously identified 975 ka horizon, three biostratigraphic datums, the 631 ka Lava Creek (Yellowstone) ash layer, and high-resolution oxygen isotopic analysis [Dean et al., in press].

2.2: Stratigraphic Interpretation

We made use of earlier work by our group on seismic stratigraphic correlation of six horizons that had been precisely dated by our suite of overlapping piston cores; the shallowest of the six was dated at ODP site 893 [Kennett, 1995; Nicholson et al 2006; Marshall et al. 2012, Dean et al., in press](Fig. 3). Deeper horizons include horizon 5 of Yeats (1981, 1989), dated at 975 ka [Huftile and Yeats, 1995]. We also correlated the ~1.8 Ma top Lower Pico, making use of paleontology from sea floor outcrop samples compiled by Marc Kamerling [Sorlien and Kamerling, 2000], using Hoyt [1976] and other sources. MMS paleontology in wells with check shot velocity surveys is being used to cross-check the interpretation of top Lower Pico on

northwest Santa Barbara Channel. Three additional horizons were interpreted, interpolating their ages between the 975 Ma Red-8 horizon and the 710 ka LimeGreen-5 horizon.

Very high resolution seismic reflection (chirp) collected by USGS on our two research cruises in 2005 and 2008 through the core sites [Nicholson et al., 2006, 2008] were used to precisely correlate the dated reflectors to high-resolution small airgun source MCS that we also collected during the 2008 cruise [Marshall, 2012]. The horizons on these MCS profiles were then correlated to the lower resolution deep industry MCS. Some of the horizons, for example violet-3 , orange-4, and SlateBlue-6, are distinctive reflections that are easily recognizable through large parts of the study area, so "drift" of the correlation off of the sequence boundary/age horizon is unlikely over large areas. Top Lower Pico is a significant erosional unconformity, especially throughout western Santa Barbara Channel. Several of the sequence boundaries are distinctive progressively-tilted onlap surfaces and/or angular unconformities in southwest Santa Barbara Channel. These could be precisely correlated south of gassy/poor imaging offshore Gaviota. In other words, where one set of seismic stratigraphic correlation pathways were not well imaged, we used another set of correlation pathways as high-confidence controls over the interpretation in the less well-imaged areas.

2.3: Dataset Analysis - IHS Kingdom Suite

Our interpretation was carried out using interactive industry software designed for seismic reflection and well interpretation, "IHS Kingdom Suite". The aforementioned seismic reflection, bathymetric, and well data were uploaded into a Kingdom Suite interpretation project. In order to test the accuracy of the navigation for the seismic reflection data, bathymetric grids were converted to two-way travel time using an interval velocity of 1,490 m/s, and displayed on the MCS profiles. Unlike other parts of offshore California, the navigation was precise and the navigation shot-trace number correspondence accurate for all Santa Barbara Channel seismic reflection data. In order to preserve people-years of effort, the October 2014 version of the project was exported from Kingdom Suite and recreated in OpendTect. Unlike Kingdom Suite, the basic version of OpendTect does not require a contract or a license. The OpendTect version of the project is seen as insurance from too much dependence on proprietary software.

2.4: Structural and Stratigraphic Interpretation

Loop-tying techniques through MCS profiles spaced at 1 to 2 km serves as a type of error analysis. Loop-tying involves the geometrical fact that rock interfaces and faults should be at the same depth and travel time at the intersections of two planes (Fig. 4). The reality for 2D MCS data is a bit more complicated. Vertical and horizontal shifts stemming from 2D migration of dipping strata as well as the disparate resolutions of the various data sets were accounted for in the interpretations.

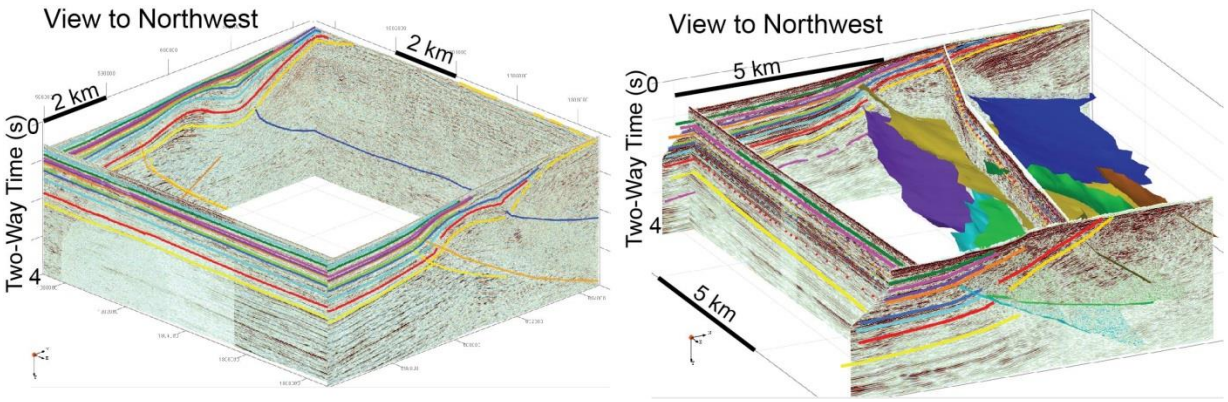

Figure 4: Stratigraphic horizon colors are the same as in Figure 3. **Left**: Fence diagram through four 2D MCS profiles, showing "ties" of 10 stratigraphic horizons and the dark blue fault at line intersections. **Right:** Two N-S inlines, one E-W crossline, and an arbitrary line through the Gato Canyon 3D MCS survey. The color surfaces are faults. A major segment boundary at a 25°+ bend in fault strike occurs within the Figure at right. The color dots on the E-W profiles are intersections of horizons interpreted on 46 N-S inlines spaced every 250 m. The color surfaces are 3D representations of N-dipping faults. Including the intersections between inlines and crosslines every 250 m that we interpreted in the 3D data sets, and the 700+ 2D profiles, and the 10 stratigraphic horizons, we made roughly 100,000 ties in Santa Barbara Channel.

Non-vertical faults can also be "tied" through intersecting strike and dip lines. Because of 2D migration effects, moderately-dipping faults can have large mis-ties between strike and dip lines, especially at deeper travel times. Fault positions were carefully interpreted on the dip lines. The faults were drawn on the strike lines through there intersections on the dips lines. Where there are strong reflections from the fault surfaces, these reflections are shallower on the strike lines than on the dip lines. Thus, on strike lines faults are interpreted through their ties from the dip lines, below their reflections. The geometrical issues are not a factor in the 3D MCS data sets because the migration is through the volume.

2.5: Gridding and Depth Conversion

Once the horizons have been interpreted, and fault interpretations were smoothed and modified for quality and consistency, 100 m two-way travel time grids were created to produce continuous surfaces. Depth-time charts from more than 3 dozen wells were constructed in Kingdom Suite. Most of these charts were derived from accurate check-shot surveys, with a few based on sonic logs. A complicated procedure within Kingdom Suite was used to produce average velocity grids to each horizon. The time grids are then converted to depth using these average velocity grids. Seven grids (each) in time and in depth were then paired, including sea surface and sea floor, with selected MCS profiles and one of the 3D volumes. This created an interval velocity model on these profiles and the 3D volume. The seismic amplitudes in travel time will be converted to amplitudes in depth.

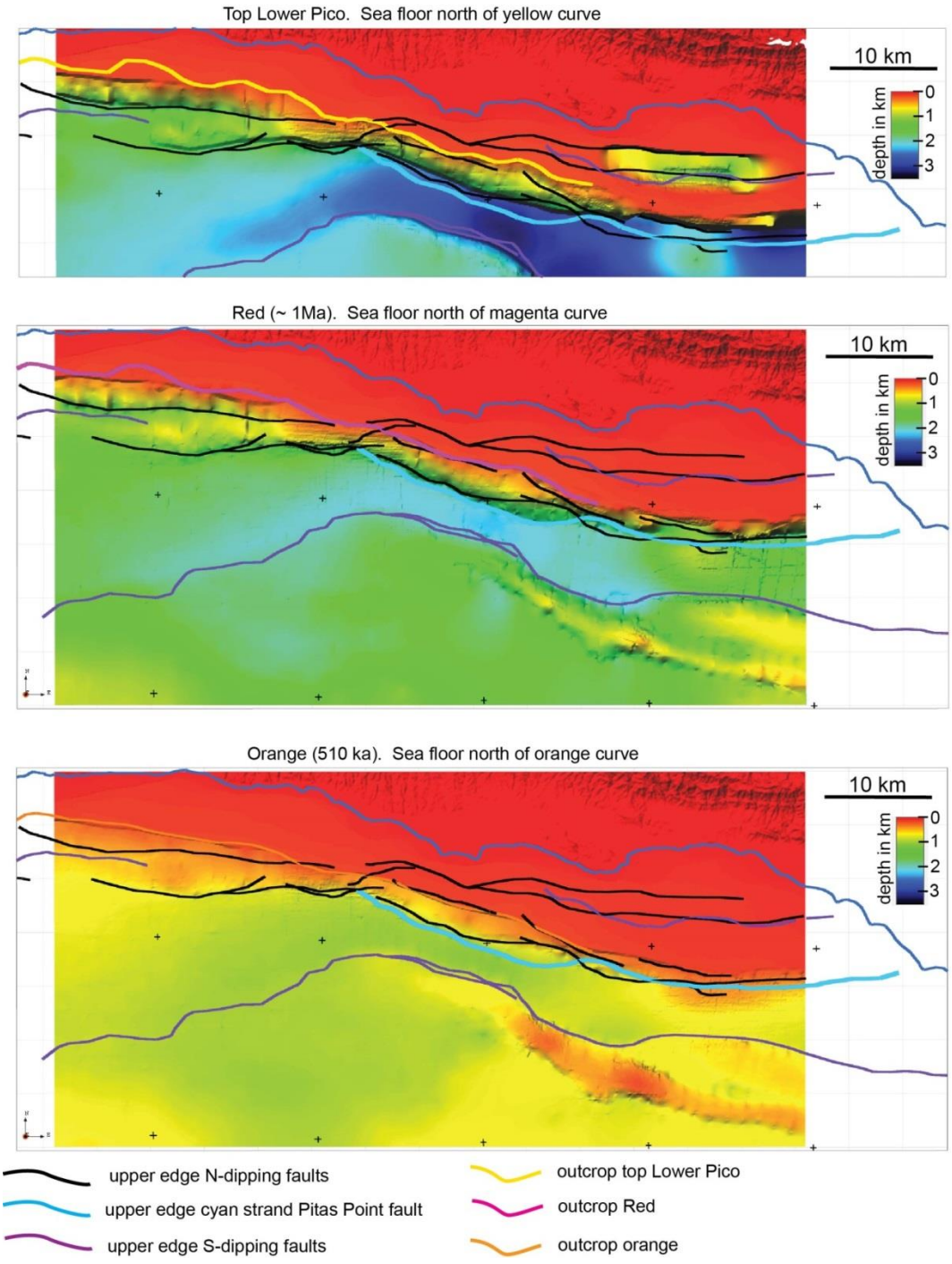

Figure 5: Depth-converted sub-bottom structure-contour grids of three of the ten interpreted horizons. The upper edges of faults are drawn, as explained in the legend. The area displayed is the part that was depth-converted: the seismic stratigraphic interpretation in travel time is over a larger area, extending to Pitas Point in the east and beyond Pt. Conception in the west (Figs. 1, 2). The sea floor and topography grid is merged with the sub-bottom grid north of its outcrop (outcrop as yellow, magenta, and orange curves).

3: Results

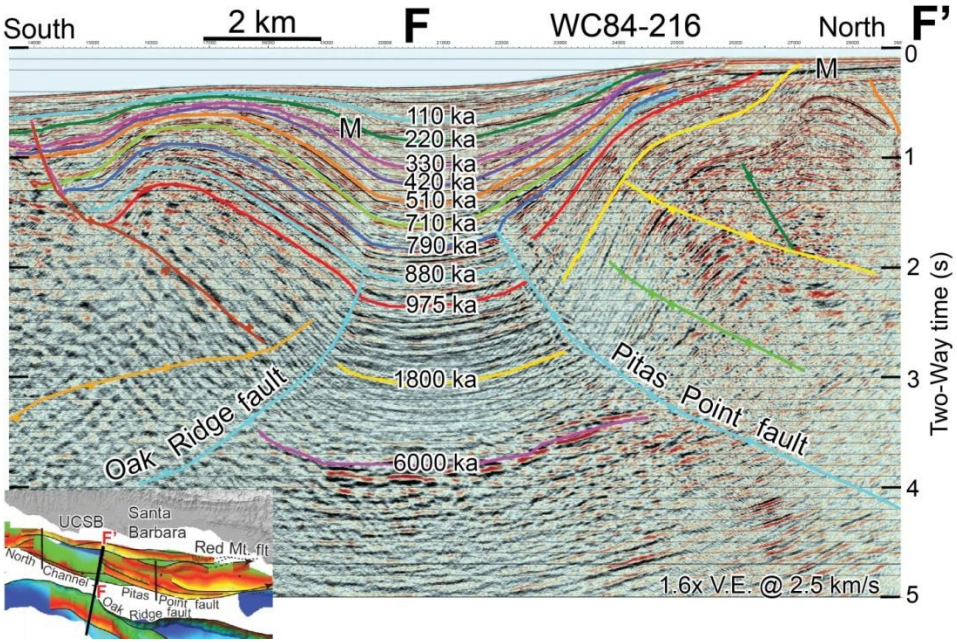

Figure 6: A 2D industry seismic reflection profile across offshore Ventura basin and the flanking fault systems. The upper part of this profile is displayed in depth in Figure 19 of Marshall (2012). "M" is the water bottom multiple reflection. Extrapolating velocity surveys in nearby wells which are as deep as 4.2 km, 4 s two-way time is at least 5.4 km depth in the basin beneath "F", and is at least 6 km depth beneath the anticline near F'.

3.1: Geometry

Our careful interpretation using all the data in Fig. 2, as explained above, resulted in digital 3D representations of many faults strands within the North Channel-Pitas Point-Red Mountain fault system (NC-PP-RM)(Fig. 6). The upper few km of this fault system continues offshore 120 km west of Ventura, to northwest of Pt. Conception (Fig. 1). There are only two important geometric segment boundaries in the upper 6 km within this 120 km-long offshore fault system. One is located 10 km west of UCSB, and the other is offshore Gaviota. The deepest interpreted main strand of the fault system, the cyan strand of the Pitas Point fault, has no significant geometric discontinuities in at least its upper 6 km for 60 km along strike. It is likely the same fault strand as the Ventura fault of Hubbard et al., [2014][e.g., Yerkes and Lee, 1987; Yerkes et al., 1987], although a right-stepping double bend occurs on this fault near Pitas Point [Johnson et al., 2013]. Therefore, the length of a single main strand of the Pitas Point-Ventura fault strand is about 75 km. The original representation of this fault strand in the SCEC Community Fault Model (CFM) provided by Kamerling et al [2003] ends only a couple of km west of UCSB. While there is a tear fault or other structural discontinuity there [Sorlien and Kamerling, 2000; S. Johnson, oral communication September 28, 2015], the western termination of the NC-PP-RM faults system in that area is not real: it is an artifact of where we stopped interpreting it in 2000, at the west edge of most of the high-quality industry data that we had access to at that time. The North Channel fault system, also called the North Channel Slope fault system, has long been mapped the length of Santa Barbara Channel [Yerkes et al., 1981; Heck, 1998; McCulloch, 1989]

Ten km west of UCSB, two strands of the Red Mountain fault dip 60°N, with the southern strand exhibiting normal-separation of early Quaternary strata (late Quaternary is missing)(X-X' on Fig. 7). There is a segment boundary in the NC-PP-RM fault system in this area, with a 25°+ bend in fault strike so that the faults to the west are not perpendicular to the shortening direction. West of this bend, the Red Mountain fault strands merge with the underlying blind faults dipping 25° N (D-D' on Fig. 7). A right-stepping en-echelon pattern on the sea floor [Plate 2 in Johnson et al., 2014] is imaged west of the termination of the shallow part of the northern strand, consistent with left-lateral shear. A component of left-lateral strike-slip motion is thus expected on the underlying gently-dipping blind faults (also oral communication R. Heck, late 1990s).

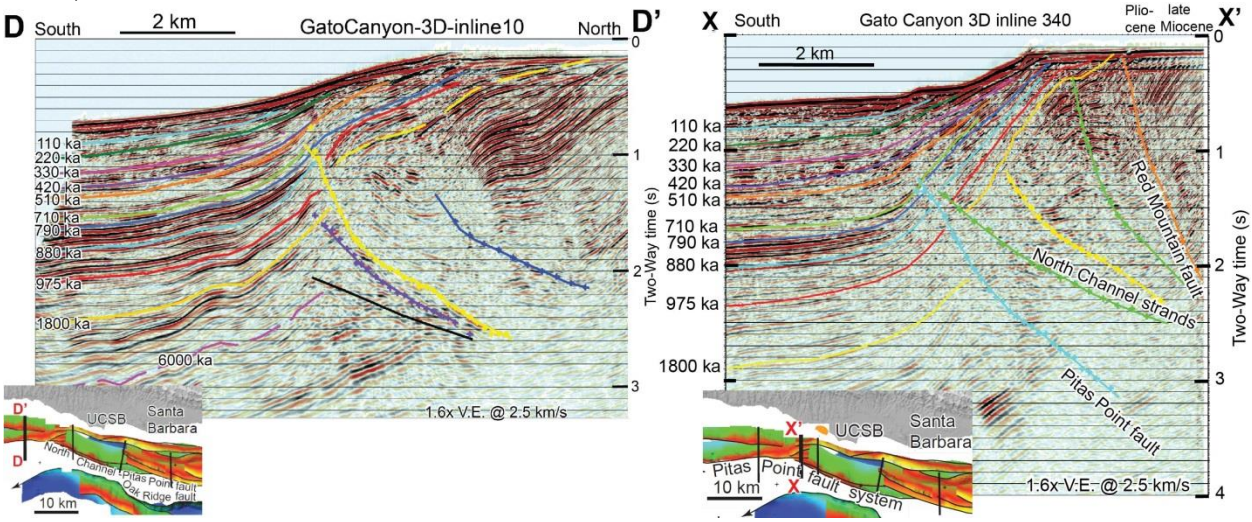

Figure 7: Vertical slices through the Gato Canyon 3D seismic reflection data volume located west of UCSB (D-D' and X-X' on Figure 1 and insets). This data set is processed to 5 s two-way time, and faults can be interpreted to 4 s, about 7 km depth, nearby. D-D' is located 8 km west of X-X'. The labeled Pitas Point fault strand (cyan) on X-X' continues 60 km east to the Ventura coast without any significant segment boundary, and farther east onshore as the Ventura fault (Fig. 1). The southern strand of the Red Mountain fault (green) has normal separation in the area; sea floor paleontology demonstrates late Miocene at the seafloor north of its northern (orange) strand, suggesting reverse separation. The inset map for X-X' shows the reverse slip focal mechanism for the M4.8 May 29 2013 earthquake; its 8 km origin depth is on the downdip projection of the Pitas Point fault [USGS, 2013]. The lower faults strike <85° on D-D' and >110° on X-X', a 25°+ bend across a segment boundary

3.2: Blind fault-related folding and distribution of slip and sea floor uplift.

Earthquake hazard is related to the spatial distribution of slip and how much slip occurs on different patches of the fault. This is important for strong ground motion, but offshore, is especially important for tsunami generation. Fault-related folds in thrust or oblique thrust fault systems absorb the slip that does not reach the surface or sea floor. In one form of fault-propagation fold models, all of the slip in an earthquake reaches the upper fault tip line, where it is transformed into folding [Suppe and Medwedeff 1990; Mitra 1990] (Fig. 8). The fault propagates upward at the slip rate, and there is no progressive tilting of the forelimb. While this model has been widely applied to structures in southern California, our interpretations indicate that important predictions of this model are not met. For example, there is progressive tilting of

the S-dipping forelimb of the anticlinal trend above the North Channel-Pitas Point fault strands for almost the entire 120 km west of Pitas Point (Figs. 6, 7, 9, 10).

The NC-PP strands are variably blind along strike, with the upper tip of the lowest main Pitas Point fault strand near 2 km depth between offshore Santa Barbara to west of UCSB (Figs. 6, 9). This fault is blind closer to 1 km depth east of Santa Barbara, and the upper tip is a only a few hundred meters depth or less within 10 km west of Pitas Point. Other gently-dipping faults above this strand cut up shallower, but may also not be propagating. Additional steeper strands of the Red Mountain fault system cut to the sea floor but may be oblique left-reverse in the east and left-lateral in the west (Figs. 2, 7). Furthermore, the lowest interpreted main fault strand has not propagated upward in the last ~700-500 ka over a wide area offshore Santa Barbara-UCSB (Figs. 7, 9, 10). Given the progressive tilt and lack of updip propagation, most the slip during most if not all recent major earthquakes should die out over several km (or more) below the upper tip. Predicting the slip distribution on the upper few km of the fault and the sea floor/surface uplift pattern is dependent on using the correct fault-related fold model.

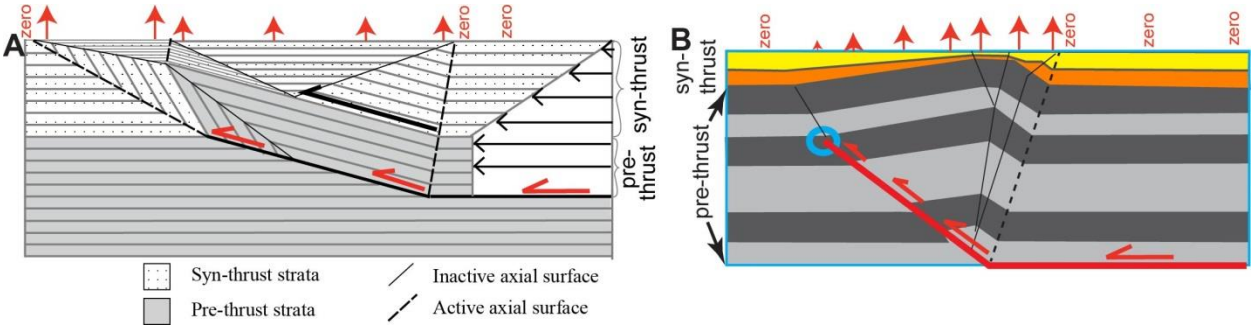

Figure 8: Models for fault related folds from Seeber and Sorlien [2000]. (A), and Sorlien et al [2013], modified from Wickham [1995] (B). Only B predicts progressive tilting of a wide forelimb, and continuously variable rates of vertical motion, rather than the steps in relative uplift seen in A. Zero means no vertical motion in a quake, and larger uplifts are shown as longer red arrows. The red half arrows along the faults are a qualitative illustration of slip magnitude during an earthquake. All the slip reaches the tip of the fault in A; the slip is absorbed by tilting over a large part of the cross-sectional fault in B. The black arrows in A give the total displacement

Forelimb dips and structural relief, although variable, are not systematically greater in the east than in the west between Carpinteria and the UCSB campus at 119° 50′ W. Farther west, the rate of tilting, and probably the rate of offshore shortening, decreases steadily through the western 40 km to the end of the system beyond Point Conception. This trend mirrors the decrease in elevation and structural relief of the Santa Ynez Mountains above the deep fault. There is no evidence of a major change in tilt rate at any one location through the last 1 Myr along the offshore fault system.

There is very strong evidence that the initiation of contraction predates deposition of the 1.8 Ma top Lower Pico horizon for the entire 120 km-long offshore fault system. The MCS data image the progressively steeper dips below top Lower Pico. These MCS data do not image very steep dips, but such steep to overturned fold limbs are seen on the Redin et al. [2005] cross sections

through wells. These cross sections indicate that the forelimb dips reach near vertical to overturned in early Quaternary rocks east of UCSB. Progressive tilts to at least moderate dips above the western fault affect Pliocene strata. These observations suggest that the entire fault system has been active in contraction since at least Pliocene time rather than propagating westward.

Uplift of the hanging wall above a thrust fault has long been used to model thrust slip in coastal areas. However, regional subsidence of the footwalls of many of these faults means that a reverse fault can be very active, yet the hanging-wall not exhibit rock uplift or surface uplift relative to an arbitrary reference datum like paleo-sea level [Pinter et al., 2003; Sorlien et al., 2006 and 2013]. It is structural relief growth, not surface uplift, which must be used for modeling of fault displacements. Figure 6, combined with evidence of older wave erosion, shows that the hanging wall of the active Oak Ridge fault has been subsiding, but more slowly than the rapidly subsiding footwall block [Nicholson et al, 2006, Hopkins, 2006; Marshall, 2012]. The regional subsidence is likely due to post-rift thermal contraction, and to sediment and tectonic loading. Related to this, the structural relief for the 1,800 and 975 ka horizons (assuming relatively small changes in paleo water depth) on G-G' (Fig. 10) is very similar to that for F-F' (Fig. 9). Yet, the shortening is much greater across G-G' than F-F'. The hanging-wall is thrusting over the subsiding footwall on G-G'. Thus, in a 10 km distance, the shortening decreases by a factor of 2, without a change in the structural relief. The depth of the upper edge of the faults increases from about 1 km (east) to 2 km (west) across this distance. The effect of subsidence on thrusting over Ventura basin is discussed in Nicholson et al. [2007].

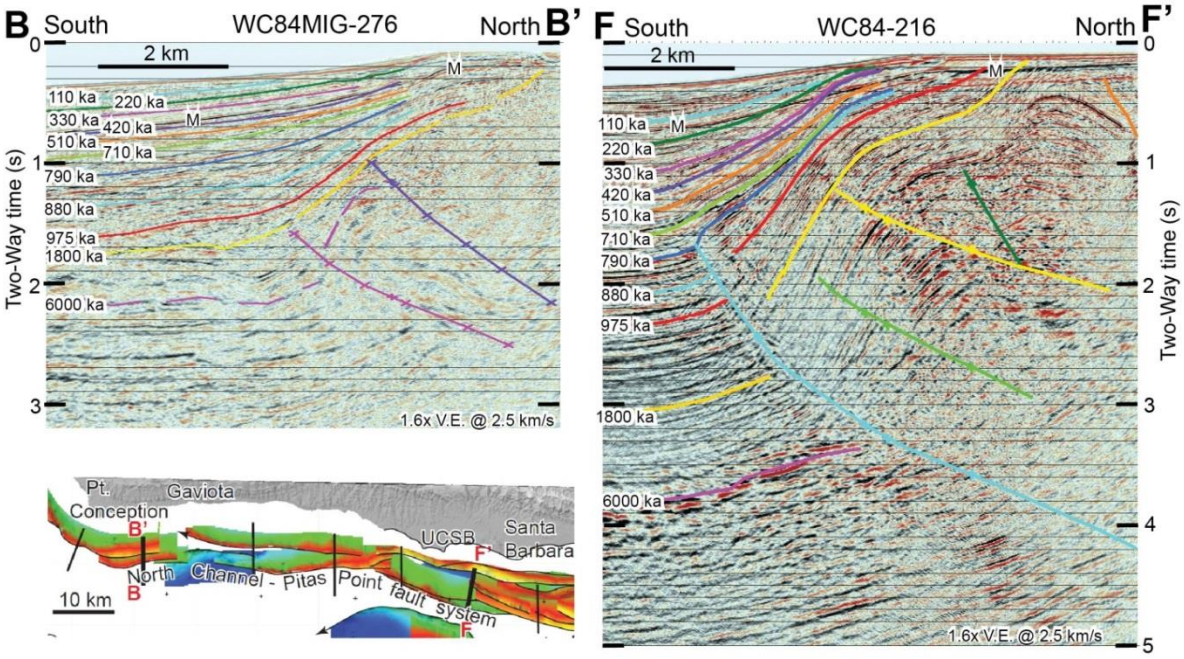

Figure 9: Western Geophysical profiles B-B' and F-F' are 65 km apart (inset map and Figure 1). Shortening, structural relief , and tilt rate are all much less at B-B' than F-F'. The part of shortening absorbed offshore increases greatly east of F-F'; compare to G-G' in Figure 10.

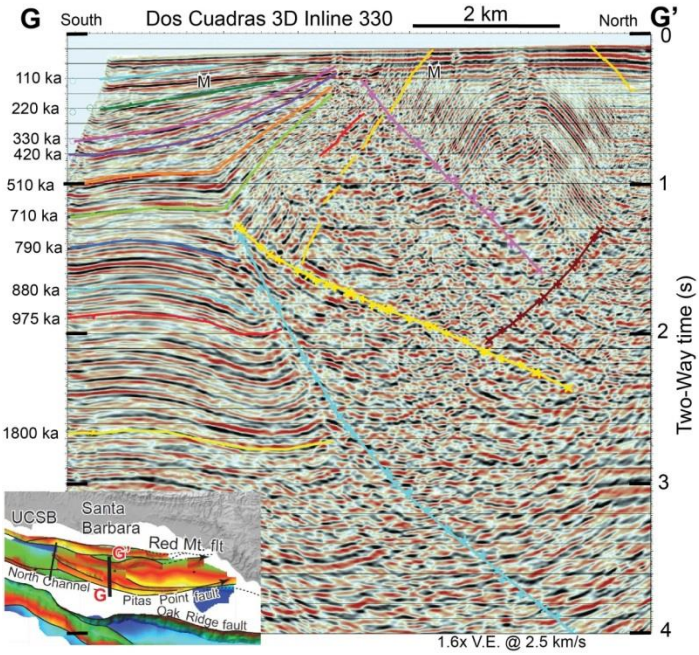

Figure 10. Inline profile from the Dos Cuadras 3D seismic reflection survey. The shortening of the 1800 ka (yellow) horizon here is about 4 km, and its structural relief after accounting for erosion is more than 3 km [Sorlien and Kamerling, 2000]. Compare to F-F' in Figure 9, which has the same structural relief but less than half the shortening.

3.2: Displacement Modeling.

We do not yet have new quantitative estimates of fault displacements and slip rates through time. The stratigraphic horizons have been depth converted using a 3D velocity model. However, depth conversion of the new 3D fault interpretation and of the seismic reflection profiles is still underway. We do, however, show a quantitative restoration of displacements and shortening in Figure 11. This is a figure from Sorlien and Kamerling [2000], produced after unfolding the top Lower Pico digital grid and fitting the flattened surfaces back together across faults [Gratier and Guillier, 1993]. Even though we have twice the 2D MCS data available compared to 2000, as well as 3D MCS surveys, our new top Lower Pico horizon map is very similar to the one in Sorlien and Kamerling [2000]. The map done in 2000 was extrapolated above the sea floor where eroded, which is necessary for a complete UNFOLD/map restoration. The new grids only exist where the horizon exists, and are merged with the seafloor where older strata outcrop. Therefore, the new grids are not yet suitable for use by the UNFOLD software.

The restoration in Figure 11 shows decreasing shortening from east to west of the footwall of the south branch of the Red Mountain fault with respect to a southern reference line. There is a particularly dramatic decrease in shortening across ~20 km east of UCSB. It is not possible to do this type of restoration for the 975 ka or younger horizons. This is because they are eroded over too large a part of the structure. Instead, we can compare the post-1800 ka displacements to the deformation of the S-dipping forelimb of the anticlinal trend. There is no obvious change in the rate of forelimb tilting since 1,800 ka, and especially since 975 ka, on any single interpreted MCS profile.

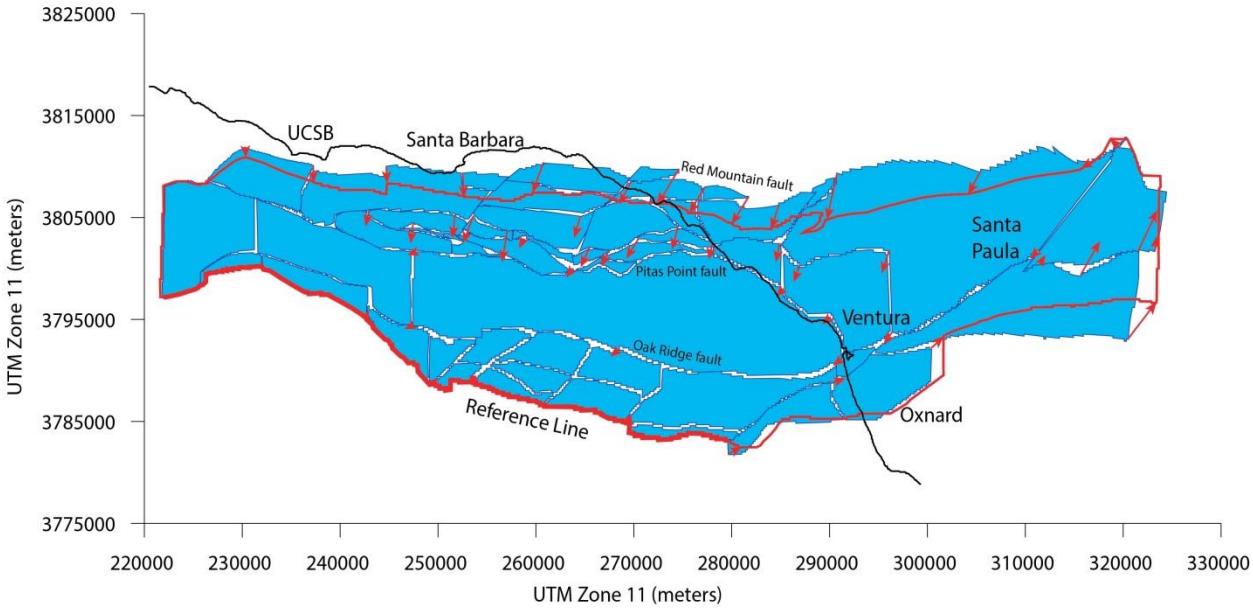

Figure 11: Map restoration of the ~1.8 Ma top Lower Pico horizon including use of UNFOLD to restore horizons within fault blocks to horizontal [Gratier and Guillier, 1993] and fitting those unfolded surfaces back together across faults with respect to the southern reference line. The axes are in meters and the red displacement arrows are at that scale. Shortening south of the Red Mountain fault is about 5 km near Ventura, and 1 km near UCSB. From Sorlien and Kamerling [2000]. This restoration produces minimum estimates of deformation because sediment compaction and pressure solution are not modeled.

4: **Discussion and Conclusions**

The North Channel –Pitas Point – Red Mountain fault system continues 120 km west of Ventura. A single main strand, the Pitas Point- Ventura strand, has no significant geometrical discontinuities in at least its upper 6 km for 60 km west of Pitas Point, to a significant segment boundary located 10 km west of UCSB. A fold kink above the shallow fault tip was mapped nearshore by Johnson et al. [2013], through a double bend (Fig. 1). Our new fault interpretation is very similar to the one of Kamerling et al. [2003], which has long been available in the SCEC Community Fault Model [Plesch et al., 20007]. The Kamerling et al. [2003] representation was based on wells, still-proprietary industry 2D seismic reflection data, and relocated seismicity.

Hubbard et al. [2014] produced a representation of a single N-dipping Ventura fault onshore based on onshore petroleum well data, and limited onshore seismic reflection. This onshore fault representation has been criticized as at best incomplete [Nicholson et al., 2015; see also Hopps et al., 1992 and Grigsby, 1986]. The fault geometry derived from onshore data was then projected/extrapolated 30 km offshore to Santa Barbara [Hubbard et al., 2014]. It does not include the western 30 km of this fault strand to the segment boundary, or the 3D geometry of the offshore faults as derived from petroleum wells, MCS data, and seismicity data [e.g., Kamerling et al., 2003]. The Hubbard et al. [2014] fault representation has been added to the SCEC CFM in version 5.0, to supplement the Kamerling et al. [2003] version.

Abundant well data and clear imaging using 2D and 3D seismic reflection data show offshore S-dipping fault(s) above the N-dipping North Channel-Pitas Point fault strands (Fig. 10)[Edwards,

1998; Sorlien and Kamerling, 2000; Kamerling et al., 2003; Redin et al., 2005]. This fault is not in the SCEC CFM 4.0, but portions of the S-dipping fault are now being incorporated into CFM version 5.0. The existence of this very young blind fault complicates any rupture model.

The new addition to the SCEC CFM, the N-dipping extrapolated upper ramp fault geometry for the Pitas Point (Ventura) fault from Hubbard et al. [2014], was used for tsunami modeling of an average 7.4 m, maximum ~15 m slip offshore thrust earthquake, with most of the slip reaching the sea floor [Ryan et al., 2015]. Sea floor uplift reaches a maximum of 10-12 m in that model earthquake. This is not consistent with the high-resolution and deeper penetration seismic reflection data indicating that the offshore fault does not reach the sea floor (Fig. 10)[Sorlien and Kamerling, 2000; Redin et al., 2005; Edwards, 1998; Johnson et al., 2013]. The upper tip of the fault is at a few hundred meters or less depth within 10 km of Pitas Point, is at about 700 m depth for 20 km east of Santa Barbara, and is at about 2 km depth west of Santa Barbara. Just as important, the main lower strand of the Pitas Point fault has not been propagating for the last 500 to 700 ka. This is consistent with the observed progressive tilting (horizontal axis limb rotation) of the forelimb for the entire 120 km offshore fault-fold system, but not consistent with the model results of fault slip reaching the seafloor. Most slip in an earthquake in this type of fault-fold system will not reach the upper fault tip, and may die out gradually updip across several km of the fault (Fig. 8) [K. Johnson et al., 2015]. We suggest that shallow slip was overestimated in Ryan et al [2015] and an emergent fault does not exist in the area of the modeled offshore earthquake. In contrast to our suggestion that shallow fault slip in earthquakes is far less than modeled, the length of model worst-case offshore ruptures should greater. There is no large segment boundary at Santa Barbara, and this Pitas Point (Ventura) fault strand continues 30 km farther west to an important segment boundary (Fig. 1).

The SCEC CFM does not include information from the people generating the fault representation on limitations of the digital faults, and there is no information in the CFM concerning the folding above blind faults, and thus of the possible inferred slip distribution in earthquakes. There are also multiple alternate, incomplete, and to some extent, mutually incompatible representations of the same fault in the CFM. It seems unlikely that a modeler can make the best use of the CFM without communicating with the different people who have worked on the different representations.

The entire length of the offshore North Channel – Pitas Point fault system was active in contraction/transpression long before 1800 ka. Therefore, not only have parts of it not been propagating updip, but the system has not propagated laterally during Quaternary time as far west as Pt. Conception. The lower offshore shortening in the west is due to slower rates of deformation and not to a younger fault system.

5.0: Data availability

Much of the seismic reflection data are available from the USGS NAMSS web site [Hart and Childs, 2005]. The bathymetry data are also publicly available as described in the text. The digital fault surfaces are now being converted to depth. These fault surfaces will be provided to Craig Nicholson and Andreas Plesch for incorporation into the SCEC Community Fault Model. This report will be modified for publication, at which time the stratigraphic interpretation will be included as a supplement. Horizon grids in both time and in depth represent the 3D velocity model. P.I. Sorlien has been releasing seismic stratigraphic interpretations as supplements to

publications [Sorlien et al., 2013, 2015; Kurt, Sorlien et al. 2013]. As noted in the caption to Figure 2, much of the Kingdom Suite interpretation project has been provided to Samuel Johnson of the Santa Cruz California USGS office. An additional Kingdom Suite project representing multiple people-years of work, covering from Santa Monica Bay to the Mexican border, was also provided to that Santa Cruz office as well as to the USGS water resources office in San Diego.

6.0: Acknowledgments: We acknowledge the support of Paradigm for the discounted use of Gocad and IHS for the donation of The Kingdom Suite software. OpendTect, made available by dGB Earth Sciences, was also used. The authors acknowledge WesternGeco, Chevron, and the U.S. Geological Survey for providing the seismic reflection data for the purpose of this research. Richard Behl and James Kennett did much of the work to produce the stratigraphic age model, based on 740 ka and younger core material. Marc Kamerling provided recent scientific discussion and we made use of his early 2000s work. Samuel Johnson participated in scientific discussion of the science in this report.

7.0 References

Behl, R.J., S. Afshar, J. P. Kennett, C. Nicholson, C. C. Sorlien, C. D. Marshall, T. M. Hill, S. M. White, W. E. Dean, and J. A. Barron, "Extending the Record of Abrupt and Millennial-Scale Climate and Ocean Change Through the Mid-Pleistocene Transition in Santa Barbara Basin, California", (2011). Conference Proceedings, Published Bibliography: 25th Pacific Climate Workshop (PACLIM), Monterey, CA.

Dartnell, P., G. Cochrane, and M. E. Dunaway, 2005, Multibeam bathymetry and backscatter data: northeastern Channel Islands region, southern California, U. S. Geological Survey Open-File Report 2005-1153, Version 1.0, http://pubs.usgs.gov/of/2005/1153/

Dean, W. E., J. P. Kennett, R. J. Behl, C. Nicholson, and C. C. Sorlien, Abrupt termination of Marine Isotopic Stage 16 (Termination VII) at 631.5 ka in Santa Barbara basin, California, in press, Paleoceanography.

Dibblee, T.W. Jr., 1950, Geology of southwestern Santa Barbara County, California, California Division of Mines and Geology Bulletin 150, 95 p.

Dibblee,T.W. Jr., 1966, Geology of the central Santa Ynez Mountains, Santa Barbara, California, Calif. Div. Mines and Geology, Bull. 186, 99 p.

Dolan, J. F., D. D. Bowman, and C.G. Sammis (2007). "Long-range and long-term fault interactions in Southern California." Geology 35(9) 855-858.

Edwards, E. B., 1998, Redevelopment of the Carpinteria Field, Santa Barbara Channel, California, Structure and Petroleum Geology, Santa Barbara Channel, California, MP 46, eds.: D. S. Kunitomi, T. E. Hopps, and J. M. Galloway, Pacific Section Amer. Assoc. Petrol. Geol., Bakersfield, California, p. 239-246.

Eichhubl, P., H. G. Greene, and N. Mahler, 2002, Physiography of an active transpressive margin basin: high-resolution bathymetry of the Santa Barbara basin, Southern California continental borderland, Marine Geology, 184, 95-120.

Fisher, M. A., C. C. Sorlien, and R. W. Sliter, 2009, Potential earthquake faults offshore Southern California, from the eastern Santa Barbara Channel south to Dana Point, in H. J. Lee and W.

R. Normark, eds., Earth Science in the Urban Ocean: The Southern California Continental Borderland: Geological Society of America Special Paper 454, p. 271-290, doi: 10.1130/2009.2454(4.4).

Gamble, L., 1983, The organization of artifacts, features, and activities at Pitas Point: A coastal Chumash village. Journal of California and Great Basin Anthropology, 5, (1), 103-129.

Grigsby, F. B., 1986, Quaternary tectonics of the Rincon and San Miguelito oil fields area, western Ventura basin, California, M.S. thesis, 110 pages, Oregon State University, Corvallis.

Gratier, J.-P., and B. Guillier, 1993, Compatibility constraints on folded and faulted strata and calculation of total displacement using computational restoration (unfold program), Journal of Structural Geology, J. G. Ramsay Special Issue, vol. 15, p. 391-402.

Hart, P. E., and J. R. Childs (2005), National archive of marine seismic surveys (NAMSS): Status report on U. S. Geological Survey program providing access to proprietary data, Eos Trans. AGU, 86(18), Jt. Assem. Suppl., Abstract S41A-10.

Heck, R. G., 1998, Santa Barbara Channel regional formline map, top Monterey Formation, in: Structure and Petroleum Geology, Santa Barbara Channel, California, MP 46, eds.: D. S. Kunitomi, T. E. Hopps, and J. M. Galloway, Pacific Section American Association of Petroleum Geologists, Bakersfield, California, p. 183-184, plate I.

Heck, R.G., and E. B. Edwards, 1998, Gato Canyon field, Santa Barbara Channel, California, in: Structure and Petroleum Geology, Santa Barbara Channel, California, MP 46, eds.: D. S. Kunitomi, T. E. Hopps, and J. M. Galloway, Pacific Section American Association of Petroleum Geologists, Bakersfield, California, p. 293-299.

Hopkins, S.E., Geometry and Quaternary evolution of the Oak Ridge fault system, Santa Barbara Channel, California, Master's Thesis, University of California, 55 pp., 2006.

Hopps, T.E., H. E. Stark, and R. J. Hindle, 1992, Subsurface geology of Ventura Basin, California, Ventura Basin Study Group Report, 45 pp., 17 structure contour maps and 84 structure panels comprising 21 cross sections, Rancho Energy Consultants, Inc., Santa Paula, CA. http://projects.eri.ucsb.edu/hopps/.

Hoyt, D. H., 1976, Geology and recent sediment distribution from Santa Barbara to Rincon Point, California: M. S. thesis, San Diego State University, 91 p.

Hubbard, J., J. H. Shaw, J. Dolan, T. L. Pratt, L. McAuliffe, and T. K. Rockwell, 2014, Structure and seismic hazard of the Ventura Avenue anticline and Ventura fault, California: Prospect for large, multi-segment ruptures in the Western Transverse Ranges, Bull. Seismol. Soc. Amer. 104, doi: 10.1785/0120130125.

Huftile, G. J., and R. S. Yeats (1995), Convergence rates across a displacement transfer zone in the western Transverse Ranges, Ventura basin, California, J. Geophys. Res., 100, 2043-2067.

Johnson, K. M., 2015, Growth of fault-propagation folds by flexural slip folding: Implications for Earthquakes, poster SDOT-226, Proceedings Volume XXV, Southern California Earthquake Center Annual Meeting, September 12-16, Palm Springs, California. https://www.scec.org/sites/default/files/SCEC2015Proceedings.pdf.

Johnson, S.Y., Dartnell, P., Cochrane, G.R., Golden, N.E., Phillips, E.L., Ritchie, A.C., Kvitek, R.G., Greene, H.G., Krigsman, L.M., Endris, C.A., Seitz, G.G., Gutierrez, C.I., Sliter, R.W., Erdey, M.D., Wong, F.L., Yoklavich, M.M., Draut, A.E., and Hart, P.E. (S.Y. Johnson and S.A.

Cochran, eds.), 2013, California State Waters Map Series—Offshore of Ventura, California: U.S. Geological Survey Scientific Investigations Map 3254, pamphlet 42 p., 11 sheets, available at http://pubs.usgs.gov/sim/3254/.

Johnson, S.Y., Dartnell, P., Cochrane, G.R., Golden, N.E., Phillips, E.L., Ritchie, A.C., Kvitek, R.G., Dieter, B.E., Conrad, J.E., Lorenson, T.D., Krigsman, L.M., Greene, H.G., Endris, C.A., Seitz, G.G., Finlayson, D.P., Sliter, R.W., Wong, F.L., Erdey, M.D., Gutierrez, C.I., Leifer, I., Yoklavich, M.M., Draut, A.E., Hart, P.E., Hostettler, F.D., Peters, K.E., Kvenvolden, K.A., Rosenbauer, R.J., and Fong, G. (S.Y. Johnson and S.A. Cochran, eds.), 2014, California State Waters Map Series—Offshore of Coal Oil Point, California: U.S. Geological Survey Scientific Investigations Map 3302, 57 p., 12 sheets, scale 1:24,000, available at http://dx.doi.org/10.3133/sim3302.

Johnson, S.Y., Dartnell, P., Cochrane, G.R., Golden, N.E., Phillips, E.L., Ritchie, A.C., Krigsman, L.M., Dieter, B.E., Conrad, J.E., Greene, H.G., Seitz, G.G., Endris, C.A., Sliter, R.W., Wong, F.L., Erdey, M.D., Gutierrez, C.I., Yoklavich, M.M., East, A.E., and Hart, P.E. (S.Y. Johnson and S.A. Cochran, eds.), 2015, California State Waters Map Series—Offshore of Refugio Beach, California: U.S. Geological Survey Scientific Investigations Map 3319, pamphlet 42 p., 11 sheets, scale 1:24,000, doi:10.3133/sim33 and http://pubs.usgs.gov/sim/3319/19.

Kamerling, M. J., C. C. Sorlien and C. Nicholson (2003), 3D development of an active oblique fault system, northern Santa Barbara Channel, California, Seismol. Res. Lett., v. 74, n.2, p. 248.

Kennett, J. P., 1995, Latest Quaternary benthic oxygen and carbon isotope stratigraphy: Hole 893A, Santa Barbara Basin, California, in Kennett, J. P., and Baldauf, J., and Lyle, M., eds., Proceedings of the Ocean Drilling Program, Scientific Results, v. 146 (Part II), p. 3-18

Kurt, H., C. Sorlien, L. Seeber, M. Steckler, D. Shillington, G. Cifci, M.-H. Cormier, J.-X. Dessa, O. Atgin, D. Dondurur, E. Demirbag, S. Okay, C. Imren, S. Gurcay and H. Carton, Steady late Quaternary slip rate on the Cinarcik section of the North Anatolian fault near Istanbul, Turkey, 2013, Geophysical Research Letters, 40, doi: 0.1002/grl.50882.

Marshall, C. J. (2012), Sedimentation in an active fold and thrust belt, from 1 Ma to present, Santa Barbara Channel, California, M.S. thesis, Dept. of Geol., California State Univ. Long Beach, Long Beach, California. http://pqdtopen.proquest.com/abstract?dispub=1507771

Marshall, C. J., C. C. Sorlien, C. Nicholson, R. J. Behl, and J. P. Kennett, 2012, Sedimentation in an active fold and thrust belt, Santa Barbara Basin, CA: Local, Regional, and Global influences on the spatial and temporal evolution of sedimentation from 1.0 Ma to present, AAPG annual Meeting, April 2012, Long Beach

Marshall, S. T., G. J. Funning, and S. E. Owen (2013), Fault slip rates and interseismic deformation in the western Transverse Ranges, California, J. Geophys. Res. Solid Earth, 118, doi:10.1002/jgrb.50312.

McCulloch, D. S., (1989), Geologic map of the south-central California continental margin, eds. H. G. Greene and M. P. Kennedy, California Continental Margin Geoogic Map Series, California Dept. Mines and Geology, scale 1:250,000.

Mitra, S., 1990, Fault-propagation folds: geometry, kinematic development, and hydrocarbon traps, American Association of Petroleum Geologists v. 74, no. 6, p. 921-945

Nicholson, C., M. J. Kamerling, C. C. Sorlien, T. E. Hopps, and J.-P. Gratier, Subsidence, compaction and gravity-sliding: Implications for active 3D geometry, dynamic rupture, and seismic hazard of active basin-bounding faults in southern California, Bull. Seismo. Soc. Amer., 97 p. 1607-1620; DOI: 10.1785/0120060236.

Nicholson, C., J. Kennett, C. Sorlien, S. Hopkins, R Behl, W. Normark, R. Sliter, T. Hill, D. Pak, A. Schimmelmann, K. Cannariato, and the SBCore team (2006), Santa Barbara Basin study extends global climate record, Eos (Trans. Amer. Geophys. Union), 87, n.21, p.205, 208.

Nicholson, C., J.P. Kennett, R.J. Behl, C.C. Sorlien, and C.J. Marshall, Using active tectonics to extend the ultra-high-resolution global climate record from Santa Barbara Basin back to ~1.2 Ma, Eos (Transactions of AGU), 89 (53), Abstract PP11B-1390 (2008).

Nicholson, C, C. C. Sorlien, T. E. Hopps, and A. G. Sylvester, 2015, Anomalous Uplift at Pitas Point, California: Whose fault is it anyway?, Poster USR-221, Proceedings Volume XXV, Southern California Earthquake Center Annual Meeting, September 12-16, Palm Springs, California. https://www.scec.org/sites/default/files/SCEC2015Proceedings.pdf.

Pinter, N., C. C. Sorlien, and A. T. Scott, 2003, Fault-related fold growth and isostatic subsidence, California Channel Islands, Amer. J. Science, v. 303, p. 300-318.

Plesch, A, J. H. Shaw, C. Benson, W. A. Bryant, S. Carena, M. Cooke, J. Dolan, G. Fuis, E. Gath, L. Grant, E. Hauksson, T. Jordan, M. Kamerling, M. Legg, S. Lindvall, H. Magistrale, C. Nicholson, N. Niemi, M. Oskin, S. Perry, G. Planansky, T. Rockwell, P. Shearer, C. Sorlien, M. P. Suss, J. Suppe, J. Treiman, and R. Yeats, Community Fault Model (CFM) for southern California, Bull. Seism. Soc. of Amer., 97, p. 1793-1802, doi: 10.1785/0120050211.

Redin, T., J. Forman and M. J. Kamerling, 2005, Santa Barbara Channel structure and correlation sections, CS-32 through CS-42, Pacific Section AAPG, Bakersfield, CA.

Rockwell, T., K. Wilson, L. Gamble, M. Oskin, and E. Haaker, 2014, Great Earthquakes in the western Transverse Rages of southern California on the Pitas Point-Ventura thrust system, 5th International INQUA Meeting on Paleoseismology, Active Tectonics and Archeoseismology (PATA), 21-27 September 2014, Busan, Korea.

Ryan, K. J., E. L. Geist, M. Barall, and D. D. Oglesby (2015), Dynamic models of an earthquake and tsunami offshore Ventura, California, Geophys. Res. Lett., 42, doi:10.1002/2015GL064507.

Ryan, W. B. F., S. M. Carbotte, J. O. Coplan, S. O'Hara, A. Melkonian, R. Arko, R. A. Weissel, V. Ferrini, A. Goodwillie, F. Nitsche, J. Bonczkowski, and R. Zemsky (2009), Global Multi-Resolution Topography synthesis, Geochem. Geophys. Geosyst., 10, Q03014, doi:10.1029/2008GC002332, http://www.geomapapp.org/.

Scholz, C., 1990, The mechanics of earthquakes and faulting: Cambridge, United Kingdom, Cambridge University Press, 439 p.

Seeber, L, and C. C. Sorlien, 2000, Listric thrusts in the western Transverse Ranges, California, Geol. Soc. Amer. Bull., 112, p. 1067-1079.

Sliter, R. W., P. J. Triezenberg, P. E. Hart, A. E. Draut, W. R. Normark, and J. E. Conrad, 2008, High resolution chirp and mini-sparker seismic reflection data from the southern California continental shelf—Gaviota to Mugu Canyon: U.S. Geological Survey Open-File Report 2008–1246, available at http://pubs.usgs.gov/of/2008/1246/.

Sorlien, C. C., J. T. Bennett, M.-H. Cormier, B. A. Campbell, C. Nicholson , and R. L. Bauer, 2015, Late Miocene-Quaternary fault evolution and interaction in the Southern California Inner Continental Borderland, Geosphere, v. 11, no. X, doi: 10.1130/GES01118.1.

Sorlien, C. C., and M. J. Kamerling, 2000, Fault displacement and fold contraction estimated by unfolding of Quaternary strata, onshore and offshore Ventura basin, California, Final Report to U.S. Geological Survey NEHRP, contract 99HQGR0080.

Sorlien, C. C., M. J. Kamerling, L. Seeber, and K. G. Broderick, 2006, Restraining segments and reactivation of the Santa Monica–Dume–Malibu Coast fault system, offshore Los Angeles, California, J. Geophys. Res., 111. doi:10.1029/2005JB003632.

Sorlien, C. C., L. Seeber, K. G. Broderick, B. P. Luyendyk, M. A. Fisher, R. W. Sliter, and W. R. Normark, 2013, The Palos Verdes Anticlinorium along the Los Angeles, California coast: Implications for underlying thrust faulting, Geochemistry, Geophysics, Geosystems. http://onlinelibrary.wiley.com/doi/10.1002/ggge.20112/pdf, DOI: 10.1002/ggge.20112.

Suppe, J., and D. A. Medwedeff, 1990, Geometry and kinematics of fault-propagation folding, Eclogae geol. Helv. 83/3 p. 409-454.

USGS (2013), http://earthquake.usgs.gov/earthquakes/eventpage/ci15350729technical

Wickham, J., 1995, Fault displacement-gradient folds and the structure at Lost Hills, California (U.S.A.), J. Structural Geol., 191, p. 1293-1302, 10.1016/0191-8141(95)00029-D

Yeats, R. S., 1981, Deformation of a 1 Ma Datum, Ventura Basin, California: U. S. Geological Survey, Technical Report, Contract No. 14-08-0001-18283.

Yeats, R. S., 1989, Oak Ridge fault, Ventura basin, California, U. S. Geological Survey Open File Report OFR 89-343, 30 p.

Yerkes, R.F., H. G. Greene,J. C. Tinsley, and K. R. Lajoie, 1981, Seismotectonic setting of the Santa Barbara Channel area, southern California: USGS map MF-1169 and accompanying report.

Yerkes, R. F. and W. H. K. Lee,1987, Late Quaternary deformation in the Western Transverse Ranges, in: Recent Reverse Faulting in the Transverse Ranges, California, U.S.G.S. Professional Paper 1339, p. 71-82.

Yerkes, R. F., A. M. Sarna-Wojcicki, and K. R. LaJoie, 1987, Geology and Quaternary deformation of the Ventura area, in: Recent Reverse Faulting in the Transverse Ranges, California, U.S.G.S. Professional Paper 1339, p. 169-178.

8.0: Bibliography:

C. Sorlien presented a talk at USGS Santa Cruz California, April 17, 2015.

Abstracts

Nicholson, C., A. Plesch, C. Sorlien. J. Shaw, E. Hauksson, 2014, The SCEC 3D Community Fault Model (CFM-v5): An updated and expanded set of oblique crustal deformation and complex fault interaction for southern California, Abstract T31B-4584 presented at 2014 Fall Meeting, AGU, San Francisco, Calif., 15-19 Dec.

Nicholson, C, C. C. Sorlien, T. E. Hopps, and A. G. Sylvester, 2015, Anomalous Uplift at Pitas Point, California: Whose fault is it anyway?, Poster USR-221, Proceedings Volume XXV, Southern California Earthquake Center Annual Meeting, September 12-16, Palm Springs, California. https://www.scec.org/sites/default/files/SCEC2015Proceedings.pdf.

Plesch, A., C. Nicholson, C. Sorlien, J. H. Shaw, and E. Hauksson, 2014, SCEC Community Fault Model Version 5.0, Poster USR-096, Proceedings Volume XXIV, Southern California Earthquake Center Annual Meeting, September 6-10, Palm Springs, California. https://www.scec.org/sites/default/files/SCEC2014Proceedings.pdf.

Plesch, A., J. H. Shaw, C. Nicholson, C. C. Sorlien, and SCFM 2015 workshop participants, 2015, Release & Evaluation of the Statewide Community Fault Model (SCFM) Version 3.0 and Continued Updates to the SCEC CFM 5.0, Poster USR-217, Proceedings Volume XXV, Southern California Earthquake Center Annual Meeting, September 12-16, Palm Springs, California. https://www.scec.org/sites/default/files/SCEC2015Proceedings.pdf

Shaw, J. H., M. Barall, R. Burgette, J. F. Dolan, E. L. Geist, J. Grenader, T.s Gobel, W. Hammond, E. Hauksson, J. A. Hubbard, K. Johnson, Y. Levy, L. McAuliffe, S. Marshall, C. Nicholson,D. Oglesby, A. Plesch, L. Reynolds, T. Rockwell, K. J. Ryan, A. Simms, C. C. Sorlien, C. Tape, H. K. Thio, S. Ward, 2015, The Ventura Special Fault Study Area: Assessing the potential for large, multi-segment thrust fault earthquakes and their hazard implications, Talk, Proceedings Volume XXV, Southern California Earthquake Center Annual Meeting, September 12-16, Palm Springs, California. https://www.scec.org/sites/default/files/SCEC2015Proceedings.pdf.

Sorlien, C. C., C. Nicholson, R. J. Behl, M. J. Kamerling, C. J. Marshall, and J. P. Kennett, 2014, The geometry of the post-Miocene North Channel-Pitas Point Fault System including post-Miocene folding, Santa Barbara Channel, California, Poster USR-094 Proceedings Volume XXIV, Southern California Earthquake Center Annual Meeting, September 6-10, Palm Springs, California. https://www.scec.org/sites/default/files/SCEC2014Proceedings.pdf.

Sorlien, C. C., C. Nicholson, M. J. Kamerling, and R. J. Behl, 2015, Strike-slip displacement on gently-dipping parts of the Hosgri fault and fold-related relief growth patterns above the blind oblique-slip North Channel-Pitas Point-Red Mountain fault system, poster USR-220, Proceedings Volume XXV, Southern California Earthquake Center Annual Meeting,

September 12-16, Palm Springs, California.
https://www.scec.org/sites/default/files/SCEC2015Proceedings.pdf.

Related refereed publications completed during period of this project:

Dean, W. E., J. P. Kennett, R. J. Behl, C. Nicholson, and C. C. Sorlien, Abrupt termination of Marine Isotopic Stage 16 (Termination VII) at 631.5 ka in Santa Barbara basin, California, in press, Paleoceanography.

Sorlien, C. C., J. T. Bennett, M.-H. Cormier, B. A. Campbell, C. Nicholson , and R. L. Bauer, 2015, Late Miocene-Quaternary fault evolution and interaction in the Southern California Inner Continental Borderland, Geosphere, v. 11, no. X, doi: 10.1130/GES01118.1.

Sweetkind, D. S., V. E. Langenheim, S. C. Bova, K. McDougall, M. E. Tennyson, and C. C. Sorlien. Geologic and geophysical digital map database of the onshore parts of the Santa Maria and Point Conception 30' x 60' quadrangles, California, U. S. Geological Survey Scientific Investigations Map XXXX, in review.

9.0: Non-technical Summary

There is an active fault system beneath the coast from near Ventura to Santa Barbara and the University of California, Santa Barbara (UCSB), continuing westward to Pt. Conception. Magnitude ~8 earthquakes with large sea floor uplifts and large tsunamis have been proposed for the larger onshore-offshore fault system. However, earthquakes over the last 200 years have been smaller than Magnitude 7. The motion on this fault system is consistent with contraction: these are thrust faults with some lateral motion. Detailed information on faulting and folding of the offshore 50 km of this fault system between Ventura and UCSB is available in reports, theses and publications; there has been no such detailed information available for the additional 60 km between UCSB and Pt. Conception until now.

Our new work documents the complex 3D geometry of the offshore faults and folds. Sub-bottom acoustic imaging (seismic reflection data), data from petroleum wells, and precise age control from scientific core holes are the main data. One main strand of the fault system, the Pitas Point (Ventura) fault, is continuous offshore for 60 km to a significant segment boundary located 10 km west of UCSB. The onshore-offshore fault strand is 75 km-long, and probably capable of a M7+ earthquake given the large area of the fault. Larger earthquakes are possible if multiple segments rupture together. However, the offshore folding requires a different sea floor uplift pattern and magnitude than used to produce a model tsunami in a recent publication. The total contraction over the last 2 million years decreases westward, with a large decrease between Santa Barbara and UCSB. Folding suggests that the contraction rate through any interval during the last million years decreases similarly to the long-term average rate. Left-lateral strike-slip faulting along this fault-fold belt is more important west of UCSB.